Biochemical and molecular studies of atypical nevi

Nieuwpoort, A.F. van

5

Does oxidative stress drive melanoma development? – new evidence from gene ontology studies

Submitted

Frans A. van Nieuwpoort[1]

Coby Out-Luiting[1]

Femke A. de Snoo[2]

Stan Pavel[1]

Wilma Bergman[1]

Nelleke A. Gruis[1]

1) Department Of Dermatology, Leiden University Medical Centre, Leiden, The Netherlands

2) Centre for Human and Clinical Genetics Leiden University Medical Centre, Leiden, The Netherlands

Abstract

Melanoma development is characterized by subsequent transition of normal melanocytes into a nevus, clinical atypical (or dysplastic) nevus, radial and subsequently vertical growth phase melanoma. Most research focuses on cure of melanoma, by studying the molecular changes associated with advanced disease. The aim of this study is to investigate whether early melanoma development, in which a normal melanocyte progresses towards an atypical melanocyte, is already accompanied by distinctive changes in gene expression driving the progression towards melanoma. In this study we obtained gene expression data of 18 sets of short-term cultured normal and atypical melanocytes derived from the same individual. Gene ontology (GO) analysis revealed differentially expressed GO-categories (organellar ribosome (P=1x10^{-5}), mitochondrial ribosome (P=1x10^{-5}), hydrogen ion transporter activity (P=9.22x10^{-5}) and the prefoldin complex (P=3.08x10^{-4})) between normal and atypical melanocytes. These GO-categories indicate that the main difference between normal and atypical melanocytes is an altered regulation of oxidative stress in atypical melanocytes. Oxidative stress in late stage melanoma has been evidenced by various groups. Our gene expression results and earlier biochemical work underpin that elevated levels of oxidative stress are already present in atypical melanocytes representing the early stage of melanoma development. We hypothesize these elevated levels of oxidative stress to be responsible for oxidative DNA damage driving atypical melanocytes in the direction of melanoma development.

Keywords: (atypical) melanocytes, gene expression profiling, oxidative stress, gene ontology

Introduction

Cutaneous melanoma is a highly malignant tumour which originates from melanocytes, the pigment producing cells of the skin. Melanoma tumour progression is characterized by the transition of normal melanocytes into pigmented nevi which can further grow to form so called clinical atypical (or dysplastic) nevi that then progress into radial and subsequently vertical growth phase melanoma [1, 2]. The complex multistage development process of melanoma is mediated via various cellular, biochemical and molecular changes.

Histopathologic investigations show that the earliest most striking and cell biological characteristic changes occur in atypical nevi. They include proliferation and variable atypia of epidermal melanocytes, formation of irregular nests in the epidermal basal and suprabasal layers, and the interconnection (bridging) of these nests and layers [2, 3]. An additional feature of these nevi is the presence of a dermal inflammatory host response. Morphologically, atypical melanocytes exhibit alterations in melanosomes and mitochondria, similar to those observed in melanoma cells [4, 5].

Molecular changes have been predominantly studied in the late progression stages of melanoma and include inactivation of tumour suppressor genes, activation of oncogenes and defects in housekeeping genes such as DNA repair genes [6, 7]. Although the genetic alterations at the level of benign and atypical nevi are still largely unknown, they seem to primarily concentrate around mutations in the BRAF and NRAS genes [8-11] .

To date, most studies are directed at late stages of melanoma development in order to identify molecular targets to be used for the development of new treatment options [12-14]. Our interest concentrates on what drives a melanocyte to become a melanoma.

Since several candidate gene approaches have only revealed infrequent genetic alterations for early phases of melanoma development [8-11], we now aim at identifying changes in global gene expression reflecting unknown genetic or epigenetic alterations accompanying early progression of melanoma development.

Gene expression analysis with the Affymetrix U133 Plus v2.0 Array and subsequent gene ontology analysis on 18 sets of normal and atypical melanocytes derived from the same individual, did not reveal excessive differential expression in specific genes but clearly demonstrated differential expression of genes in pathways involved in the management of oxidative stress. These findings underpin our earlier biochemical work showing that atypical melanocytes suffer from chronic oxidative stress [5, 15]. We now hypothesize that the earlier observed oxidative stress caused by pheomelanin synthesis together with insufficient management of oxidative stress may lead to oxidative DNA damage that could be till today an underestimated prerequisite for melanoma development.

Materials and Methods

Cell cultures

Eighteen atypical nevi were excised widely with written consent from patients and Institutional Review Board approval of the Leiden University Medical Center. From the most atypical part of the excised atypical nevus a small biopsy was taken, dehydrated and embedded in paraffin according to standard histological protocols. A 7 µm section was cut and a HE staining was performed and reviewed by a pathologist for confirmation of atypia and exclusion of primary melanoma of the excised lesion.

Fat tissue was discarded and normal tissue surrounding the widely excised atypical nevus was removed for the purpose of normal melanocyte culture. Both the normal tissue and remaining atypical part of the nevus were incubated with trypsin o/n at 4 °C. The following day the epidermis and dermis from both parts were separated, collected and resuspended in cell culture medium (Hams F10 with penicillin (100 U/ml), streptomycin (100U/ml), L-glutamine (all obtained from Invitrogen, Breda, The Netherlands), 1% Ultroser G (Biosepra, Cipbergen inc, Fremont California, USA) including the following growth factors: Endothelin-1 (5 ng/ml), basic-FGF (5 ng/ml), Cholera toxin (30 µg/ml), IBMX (33 µM) and 8 nM TPA (all obtained from Sigma Aldrich, Zwijndrecht, The Netherlands). Both the melanocytes obtained from the surrounding skin as from the atypical nevus part were cultured in the same culture medium for a maximum of 5 passages and were collected while being in the log-phase to minimize differences due to cell cycle effects.

RNA isolation and sample preparation for microarrays

Approximately 5 million (atypical) melanocytes were used per RNA isolation. Directly after harvesting of the cells, total RNA was isolated using the Qiagen RNA easy kit (Qiagen, Venlo, Netherlands). The collection and purification of the RNA was done according to the manufacturer's instructions.

However to make sure the pigment was removed from the sample, the RNA collected from the first isolation was used for a second purification after which the RNA concentration was measured in a spectrophotometer.

Using the MessageAMP^{tm} II aRNA kit from Ambion (Austin, Texas, USA) the RNA was amplified and transformed into aRNA according to the manufacturer's instructions. The aRNA was fragmented and presented to the Human Genome U133 Plus v2.0 Array from Affymetrix (Affymetrix Inc., Santa Clara, CA) using the manufacturer's protocol. With this array 54675 probe sets per sample of the 18 sets of normal and atypical melanocytes were analyzed. These probe sets were derived from Genebank, dbEST and RefSeq. The arrays were scanned using a Genechip Scanner 3000.

Data Analysis

After retrieving the data for the 18 sets of normal and atypical melanocytes and after performing normalisation by the Affymetrix software GCOS v1.2 the average fluorescence intensity was measured and globally scaled to a target value of 200. For the analysis of the microarrays the following programs were used: Spotfire (Spotfire, U.S.A, MA) and BRB-ArrayTools (Dr. Richard Simon, Biometrics Research Branch, National Cancer Institute).

Filtering and Sample Cluster Reproducibility and Significance

Expression values across the 54,657 probe sets or genes were calculated using the Robust Multichip Average method (RMA) [16]. RMA estimates are based on a robust average of background corrected for perfect match probe intensities. Normalisation was done using quantile normalisation [17]. Expression values were transformed by taking Logarithm base 2. Genes whose expression differed by at least 1.5 fold from the median in at least 20% of all arrays were retained according the method described by Simon et al. [18].

Hierarchical clustering was used to cluster the samples by comparing their expression profiles across the whole set of genes. The R (reproducibility) index and the D (Discrepancy index) described by McShane et al. [19] were calculated to evaluate the robustness of the clusters. R = 1 means perfect reproducibility of the hierarchical clustering. R = 0 means no reproducibility of the cluster. The D index indicates how the cluster reproducibility during the determination of the R-index is in disagreement.

Class Comparison and Gene Ontology analysis

During class comparison differentially expressed genes between normal and atypical melanocytes were identified using a multivariate permutation test to obtain a median false discovery rate of 10% [20]. The test statistics used are random variance t-statistics for each gene [21]. Although t-statistics were used, the multivariate permutation test is non-parametric and does not require the assumption of Gaussian distributions.

Additional Gene ontology (GO) analysis identified groups of genes whose expression was differentially regulated among normal and atypical melanocytes according to the method described by Wright et al. and Pavlidis et al [21, 22]. By analyzing GO groups, rather than individual genes, findings among biologically related genes that reinforce each other were obtained. A GO category was considered significantly differentially regulated if the significance level was less than 0.01. We considered all GO categories representing between 5 and 100 genes on the array.

Validation of the results

cDNA synthesis

Total RNA was isolated from normal and atypical melanocytes as described above. First-strand cDNA synthesis was carried out using the the iScript^{tm} select cDNA synthesis kit (Biorad, Veenendaal, The Netherlands).

Using the program Beacon Designer 5 (Premier Biosoft, Palo Alto, USA) primers were designed to validate the gene expression differences found in the GO-analysis. In table 1 an overview of primers to validate differentially expressed genes is presented. The real-time PCR data was analyzed with the software package IQ5 optical system software v2 (Biorad, CA, USA). All real-time PCR reactions were performed on the Biorad iCycler apparatus. Expression values were normalized to U1A and are expressed as the mean of three measurements.

Results

Gene expression comparison of normal and atypical melanocytes; global changes and clustering

Gene chip analysis revealed that both the normal and atypical melanocytes have an average expression of 45% of the genes, represented by 54,675 probes on the array. Scatter plots for all comparisons between normal melanocytes (NM) and atypical melanocytes (AM) (figure 1A) indicate that there are small differences in gene expression between both cell types.

Using the 18 sets of normal and atypical melanocytes obtained from 18 patients, hierarchical clustering was performed. The results demonstrated that atypical melanocytes resemble their autologous normal counterparts more closely than they resemble the atypical melanocytes of another individual (figure 1B). To test the cluster reproducibility, the Robustness index (R-index) and the Discrepancy index were calculated. The R-index for the dendogram as shown in figure 1B is 0.997 and the Discrepancy index is 0.02. The numbers for both indexes indicate that the clusters are highly reproducible and therefore strengthen our observation that the differences between normal and atypical melanocytes are valid but small.

Gene expression comparison of normal and atypical melanocytes; GO analysis

Both the clustering and scatterplots indicate that gene expression patterns rather than expression of individual genes are more likely to discriminate between normal and atypical melanocytes. Subsequent Gene ontology analysis revealed 26 GO categories representing pathways that were significantly differentially expressed between normal and atypical melanocytes (table 2A).

Among the top 7 of the most significantly expressed GO categories are genes that are down- regulated in AM and act in the functioning of ribosomes (both in cytoplasm and mitochondria) (e.g. MRPS16, MRPS22, MRPS25, MRPS28, MRPL35, MRPL37, MRPL39, MRPL42, MRLP44, MRPL47) in the activity of hydrogen ion transport (ATP6V1E2, ATP6V1G1, COX4I1, COX7C, COX8C, MS4A12, NDUFA4L2, UCRC, UQCRB), oxidoreductase activity (CryZL1, CYB5A) and kinase regulators (such as ROPN1, SPA17, LGALS12) (table 2B). Genes of the prefoldin complex (PFDN2, PFDN5, PFDN6, VBP1, DNAJA3) were found to be up-regulated in AM.

Real-time PCR confirmation

To validate gene expression differences obtained with the GO-analysis we selected 14 genes (see table 1) being part of the top 4 GO-categories (organellar ribosome, mitochondrial ribosome, hydrogen ion transporter activity, prefoldin complex) and quantified their expression by real-time PCR in all samples. For all samples we were able to confirm the microarray results (an example for 2 selected genes from the organellar and mitochondrial ribosome GO-categories are depicted in figure 2). Relative expression of these genes as measured by real-time PCR confirmed the pattern of gene expression revealed by the microarray.

Discussion

In order to understand which changes in gene expression underlie the early progression of melanoma, we compared the genome wide expression of normal melanocytes with melanocytes from one of the earliest stage of melanoma progression, the atypical nevus. Overall our results show that the expression of genes in normal and atypical melanocytes is hardly any different. But gene ontology (GO) analysis was able to reveal differentially expressed GO-categories (organellar ribosome, mitochondrial ribosome, hydrogen ion transporter activity, prefoldin complex) between normal and atypical melanocytes.

In both the GO category organellar and mitochondrial ribosome, genes encoding for mitochondrial ribosomal proteins (MRPs) were found to be differentially expressed. In the current study, for several of the differentially expressed mitochondrial ribosomal proteins (MRPs) a role in progression to melanoma can be envisioned. MRPs regulate the energy providing electron transport chain of the cell [23,24]. Especially decreased expression of MRPS16, 22, 28 and MRPL37 as suggested for the mitochondria of atypical melanocytes could affect a proper functioning of the electron transport chain [23,25]. This malfunctioning can lead to accumulation of electrons which leak into the cytosol of the cell where they can give rise to reactive oxygen species (ROS) [24]. Other MRPs like MRPL25, MRPL42 and MRPL47 are involved in the general translation of mitochondrial proteins [24,26]. A causal relationship between a diminished translation of mitochondrial ribosomal proteins resulting in mitochondrial malfunctioning and disease has been described for several diseases like MELAS (mitochondrial myopathy, encephalopathy, lactic acidoses and stroke-like episodes), MERRF (Myoclonus epilepsy associated with ragged-red fibers) and deafness, [26].

Another differentially expressed GO class, hydrogen ion transporter activity, represents genes involved in hydrogen ion transporter activity such as NADH dehydrogenase (ubiquinone) 1, crystallin zeta (quinone reductase)-like 1, ATPase V1 and cytochrome b-5. The down-regulated expression of these genes in this GO class as observed in atypical melanocytes could affect the transport of protons over cellular and organellar membranes like mitochondria, lysosomes and melanosomes [27]. In general, a diminished transport increases the pH of cells and organelles [28]. Elevation in pH has a direct effect on the activity of many growth factors, DNA synthesis, proliferation and cell transformation [29]. With respect to melanosomes elevated pH increases the reactivity of quinones (like dopaquinones) which can lead to faster binding of the quinones to thiols (like L-cysteine), resulting in increased pheomelanogenesis [28,30].

Especially during pheomelanin production, intermediates leak out of the melanosomes which can damage the membrane of mitochondria, resulting in increased leakage of electrons into the cytosol and further accumulation of ROS [24]. Supportive observations for increased ROS levels during melanoma development are elevated levels of pheomelanin and ultra-structural morphological changes of mitochondria between normal and atypical melanocytes and melanoma [4,5,15].

Cells respond to ROS by expressing genes encoding stress proteins [31,32] such as DNAJA3, prefoldin proteins and other chaperones for which the expression was found to be up-regulated in atypical melanocytes under study. In general, stress to the cell causes protein denaturation: the protein molecule loses its native functional conformation when it unfolds. Chaperones assist the damaged protein to regain its functional conformation [33]. Up-regulation of these genes suggests that the atypical melanocytes very actively try to reduce effects induced by oxidative stress.

In general, gene expression studies on melanocytes are scarce. Most of the time, expression of normal melanocytes is used as a reference in studies to determine altered expression of genes in the late melanoma progression stages [13,14,34]. Most studies show that differences in gene expression are mainly observed in the transition of the radial growth phase melanoma (RPG) into vertical growth phase (VGP) melanoma and include genes involved in mitotic cell cycle regulation, cell proliferation, cell cycle and DNA replication.

The only comparison of gene expression between common nevi and atypical nevi was performed by Scatolini et al. [35]. Twenty-four differences in gene expression were observed, especially of genes implicated in cellular adhesion and neurogenesis. A comparison of gene expression between atypical nevi and radial growth phase melanoma revealed differentially expressed genes involved in the regulation of transcription [35].

All studies so far indicate that the gene expression differences between the clinically different lesions comprising the early stages of melanoma development are small. In our study we have shown that differences in gene expression between normal and atypical melanocytes are small but involve differences in expression of genes resulting in an altered regulation of ROS. Our findings of differentially expressed genes could partly be confirmed but were more clearly present in the advanced stages of melanoma progression [13,14,34]. The latter suggests sustainability of the observed differentially expressed GO-categories in atypical melanocytes throughout melanoma cells.

The supportive role for ROS in melanoma development becomes more and more evidenced by various groups [36-45]. Gidanian et al. showed that melanosomes derived from melanoma cells in comparison to melanocytes actively produced excessive amounts of ROS [39]. Higher intracellular levels of ROS in melanoma cells were detected by the studies by Meyskens et al. [40]. They furthermore showed that due to these elevated levels of ROS melanin itself becomes progressively more oxidized and starts to function as a pro-oxidant [41].

They also showed that oxidation of melanin can be further increased by binding of metals, such as iron. These melanin-metal complexes can be converted by the Fenton reaction thereby producing even more ROS [42]. There is supportive evidence that sustained oxidative stress is related to oxidative DNA damage [46]. Previous work from our group revealed that atypical melanocytes have increased levels of oxidative stress and oxidative DNA damage [5,15]. In line with these observations, Leikam et al. found that ROS production was accompanied by enhanced DNA damage [47]. However, whether oxidative DNA damage furthermore introduces genetic alterations leading to malignant transformation of melanocytes is however not yet clear and needs to be the subject of further study.

Acknowledgements

We thank Pieter van der Velden and Remco Dijkman for the fruitful discussions throughout this study. Prof. Mooi is acknowledged for hispathological analysis of the excised nevi. N.A.G. is a recipient of an Aspasia fellowship of the Netherlands Organisation for Scientific Research.

References

1. Greene MH, Clark WH, Jr., Tucker MA, Elder DE, Kraemer KH, Guerry D *et al.* Acquired precursors of cutaneous malignant melanoma. The familial dysplastic nevus syndrome. *N Engl J Med* 1985; **312**(2): 91-97.

2. Clark WH, Elder DE, Guerry D, Epstein MN, Greene MH, Vanhorn M. A Study of Tumor Progression - the Precursor Lesions of Superficial Spreading and Nodular Melanoma. *Human Pathology* 1984; **15**(12): 1147-1165.

3. Elder DE. Dysplastic naevi: an update. *Histopathology* 2010; **56**(1): 112-120.

4. Rhodes AR, Seki Y, Fitzpatrick TB, Stern RS. Melanosomal alterations in dysplastic melanocytic nevi. A quantitative, ultrastructural investigation. *Cancer* 1988; **61**(2): 358-369.

5. Pavel S, van Nieuwpoort F, van der Meulen H, Out C, Pizinger K, Cetkovska P *et al.* Disturbed melanin synthesis and chronic oxidative stress in dysplastic naevi. *European Journal of Cancer* 2004; **40**(9): 1423-1430.

6. Hussein MR. Genetic pathways to melanoma tumorigenesis. *J Clin Pathol* 2004; **57**(8): 797-801.

7. Hussein MR, Wood GS. hMLH1 and hMSH2 gene mutations are present in radial growth-phase cutaneous malignant melanoma cell lines and can be induced further by ultraviolet-B irradiation. *Exp Dermatol* 2003; **12**(6): 872-875.

8. Pollock PM, Meltzer PS. A genome-based strategy uncovers frequent BRAF mutations in melanoma. *Cancer Cell* 2002; **2**(1): 5-7.

9. Pollock PM, Harper UL, Hansen KS, Yudt LM, Stark M, Robbins CM *et al.* High frequency of BRAF mutations in nevi. *Nature Genetics* 2003; **33**(1): 19-20.

10. Wu J, Rosenbaum E, Begum S, Westra WH. Distribution of BRAF T1799A(V600E) mutations across various types of benign nevi: implications for melanocytic tumorigenesis. *Am J Dermatopathol* 2007; **29**(6): 534-537.

11. Thomas NE. BRAF somatic mutations in malignant melanoma and melanocytic naevi. *Melanoma Res* 2006; **16**(2): 97-103.

12. Hussein MR, Roggero E, Tuthill RJ, Wood GS, Sudilovsky O. Identification of novel deletion Loci at 1p36 and 9p22-21 in melanocytic dysplastic nevi and cutaneous malignant melanomas. *Arch Dermatol* 2003; **139**(6): 816-817.

13. Smith AP, Hoek K, Becker D. Whole-genome expression profiling of the melanoma progression pathway reveals marked molecular differences between nevi/melanoma in situ and advanced-stage melanomas. *Cancer Biol Ther* 2005; **4**(9): 1018-1029.

14. Mischiati C, Natali PG, Sereni A, Sibilio L, Giorda E, Cappellacci S *et al.* cDNA-array profiling of melanomas and paired melanocyte cultures. *J Cell Physiol* 2006; **207**(3): 697-705.

15. Smit NP, van Nieuwpoort FA, Marrot L, Out C, Poorthuis B, van PH *et al.* Increased melanogenesis is a risk factor for oxidative DNA damage--study on cultured melanocytes and atypical nevus cells. *Photochem Photobiol* 2008; **84**(3): 550-555.

16. Irizarry RA, Hobbs B, Collin F, Beazer-Barclay YD, Antonellis KJ, Scherf U *et al.* Exploration, normalization, and summaries of high density oligonucleotide array probe level data. *Biostatistics* 2003; **4**(2): 249-264.

17. Bolstad BM, Irizarry RA, Astrand M, Speed TP. A comparison of normalization methods for high density oligonucleotide array data based on variance and bias. *Bioinformatics* 2003; **19**(2): 185-193.

18. Simon R, Korn E, McShane L, Radmacher M, Wright G, Zhao Y. *Design and Analysis of Microarray Investigations*. Springer-Verlag, 2003.

19. McShane LM, Radmacher MD, Freidlin B, Yu R, Li MC, Simon R. Methods for assessing reproducibility of clustering patterns observed in analyses of microarray data. *Bioinformatics* 2002; **18**(11): 1462-1469.

20. Korn EL, Troendle JF, McShane LM, Simon R. Controlling the number of false discoveries: Application to high-dimensional genomic data. *Journal of Statistical Planning and Inference* 2004; **124**(2): 379-398.

21. Wright GW, Simon RM. A random variance model for detection of differential gene expression in small microarray experiments. *Bioinformatics* 2003; **19**(18): 2448-2455.

22. Pavlidis P, Qin J, Arango V, Mann JJ, Sibille E. Using the gene ontology for microarray data mining: a comparison of methods and application to age effects in human prefrontal cortex. *Neurochem Res* 2004; **29**(6): 1213-1222.

23. Kenmochi N, Suzuki T, Uechi T, Magoori M, Kuniba M, Higa S *et al.* The human mitochondrial ribosomal protein genes: mapping of 54 genes to the chromosomes and implications for human disorders. *Genomics* 2001; **77**(1-2): 65-70.

24. O'Brien TW. Evolution of a protein-rich mitochondrial ribosome: implications for human genetic disease. *Gene* 2002; **286**(1): 73-79.

25. Emdadul HM, Grasso D, Miller C, Spremulli LL, Saada A. The effect of mutated mitochondrial ribosomal proteins S16 and S22 on the assembly of the small and large ribosomal subunits in human mitochondria. *Mitochondrion* 2008; **8**(3): 254-261.

26. Wallace DC, Shoffner JM, Trounce I, Brown MD, Ballinger SW, Corral-Debrinski M *et al.* Mitochondrial DNA mutations in human degenerative diseases and aging. *Biochim Biophys Acta* 1995; **1271**(1): 141-151.

27. Schultz BE, Chan SI. Structures and proton-pumping strategies of mitochondrial respiratory enzymes. *Annu Rev Biophys Biomol Struct* 2001; **30**: 23-65.

28. Ancans J, Tobin DJ, Hoogduijn MJ, Smit NP, Wakamatsu K, Thody AJ. Melanosomal pH controls rate of melanogenesis, eumelanin/phaeomelanin ratio and melanosome maturation in melanocytes and melanoma cells. *Exp Cell Res* 2001; **268**(1): 26-35.

29. Madshus IH. Regulation of intracellar pH in eukaryotic cells. *J. Biochem* 1988; **250**(1):1-8

30. O'Brien PJ. Molecular mechanisms of quinone cytotoxicity. *Chem Biol Interact* 1991; **80**(1): 1-41.

31. Macario AJ, Conway de ME. Sick chaperones, cellular stress, and disease. *N Engl J Med* 2005; **353**(14): 1489-1501.

32. Macario AJ, de Macario EC. The pathology of cellular anti-stress mechanisms: a new frontier. *Stress* 2004; **7**(4): 243-249.

33. Prakash S, Matouschek A. Protein unfolding in the cell. *Trends Biochem Sci* 2004; **29**(11): 593-600.

34. Hoek K, Rimm DL, Williams KR, Zhao HY, Ariyan S, Lin AP *et al.* Expression profiling reveals novel pathways in the transformation of melanocytes to melanomas. *Cancer Research* 2004; **64**(15): 5270-5282.

35. Scatolini M, Grand MM, Grosso E, Venesio T, Pisacane A, Balsamo A *et al.* Altered molecular pathways in melanocytic lesions. *Int J Cancer* 2010; **126**(8): 1869-1881.

36. Bustamante J, Bredeston L, Malanga G, Mordoh J. Role of melanin as a scavenger of active oxygen species. *Pigment Cell Res* 1993; **6**(5): 348-353.

37. Trouba KJ, Hamadeh HK, Amin RP, Germolec DR. Oxidative stress and its role in skin disease. *Antioxid Redox Signal* 2002; **4**(4): 665-673.

38. Abdel-Malek ZA, Kadekaro AL, Swope VB. Stepping up melanocytes to the challenge of UV exposure. *Pigment Cell Melanoma Res* 2010; **23**(2): 171-186.

39. Gidanian S, Mentelle M, Meyskens FL, Jr., Farmer PJ. Melanosomal damage in normal human melanocytes induced by UVB and metal uptake--a basis for the pro-oxidant state of melanoma. *Photochem Photobiol* 2008; **84**(3): 556-564.

40. Meyskens FL Jr, McNulty SE, Buckmeier JA, Tohidian NB, Spillane TJ, Kahlon RS, Gonzalez RI. Aberrant redox regulation in human metastatic melanoma cells compared to normal melanocytes. *Free Radic Biol Med* 2001;**31**(6):799-808.

41. Meyskens FL, Jr., Farmer P, Fruehauf JP. Redox regulation in human melanocytes and melanoma. *Pigment Cell Res* 2001; **14**(3): 148-154.

42. Meyskens FL, Jr., Berwick M. UV or not UV: metals are the answer. *Cancer Epidemiol Biomarkers Prev* 2008; **17**(2): 268-270.

43. Fruehauf JP, Trapp V. Reactive oxygen species: an Achilles' heel of melanoma? *Expert Rev Anticancer Ther* 2008; **8**(11): 1751-1757.

44. Fruehauf JP, Meyskens FL, Jr. Reactive oxygen species: a breath of life or death? *Clin Cancer Res* 2007; **13**(3): 789-794.

45. Meyskens FL, Jr., Farmer PJ, Anton-Culver H. Etiologic pathogenesis of melanoma: a unifying hypothesis for the missing attributable risk. *Clin Cancer Res* 2004; **10**(8): 2581-2583.

46. Cooke MS, Evans MD, Dizdaroglu M, Lunec J. Oxidative DNA damage: mechanisms, mutation, and disease. *FASEB J* 2003; **17**(10): 1195-1214.

47. Leikam C, Hufnagel A, Schartl M, Meierjohann S. Oncogene activation in melanocytes links reactive oxygen to multinucleated phenotype and senescence. *Oncogene*. 2008;**27**(56):7070-82.

Table 1: Primer sequences of selected transcripts used in Real-Time PCR

no.	Gene	GO description	Sense Primer (5'-3')	Anti sense primer (5'-3')
1	MRPS22	Organellar ribosome	GAACTGAAGCCACCAACCTATAAG	GCTGCCTCAACTGCCTGTC
2	MRPL42	Organellar ribosome	TCCAGTCCAAAATGGAGCTT	CCACAGAAGGGTGGTAGCAT
3	MRPL47	Organellar ribosome	ACCTGGTGCTTGGAGAAGAGAC	CACATAAGGCAAGGCAAAGAATCG
4	MRPL21	Organellar ribosome	GAGCCGAGATAGCTTCCTGA	CTCCTTCCCATTGGTTCTCA
5	MRPL7	Organellar ribosome	ACGCTTTGATTGCTCGATCT	TTGCCTCTTTGAAGCGTTTT
6	MRPL10	Organellar ribosome	GCAGAACAAGGAGCATGTGA	TTTCAGCCACCATGTCTTCA
7	MRPL17	Organellar ribosome	CACTCGTGAAACTGCTCAGG	CGTCGGAATGGTACACACTG
8	NDUFS1	hydrogen ion transporter activity	TGCCCTAACCTCTAAGCCCTATG	ACTTCCAACCGCATCCATTACATC
9	NOX1	hydrogen ion transporter activity	GCCTCCATTCTCTCCAGCCTATC	CACATACTCCACTGTCGTGTTTCG
10	ACADM	Mitochondrial	AGCCTTTACTGGATTCATTGTGG	ATTCCTCTAGTATCTGAACATCGC
11	HSPD1	prefoldin complex	TACTGGCTCCTCATCTCACTCG	TGCTCAATAATCACTGTTCTTCCC
12	PSMF1	prefoldin complex	AACACCTGGGTGACTTCCAC	CCCACTGCTCATGGATAGGT
13	PSMB9	prefoldin complex	CGGGCGGGAGCACCAACC	GCAGACACTCGGGAATCAGAACC
14	PSMD10	prefoldin complex	AGGTGCTCAAGTGAATGCTGTC	TGTAGCCTCATAATGGTCCTTAGC

Table 2A: Differentially expressed GO categories between 18 sets of normal and atypical melanocytes

	GO category[1]	GO Term[2]	GO description	Number of genes	LS Permutation p-value[3]	KS Permutation p-value[4]
1	313	CC	organellar ribosome	30	1.00E-05	0.0120303
2	5761	CC	mitochondrial ribosome	30	1.00E-05	0.0120303
3	15078	MF	hydrogen ion transporter activity	94	9.22E-05	9.01E-05
4	16272	CC	prefoldin complex	13	0.0003082	0.001475
5	8603	MF	cAMP-dependent protein kinase regulator activity	9	0.0006046	0.0080679
6	4164	MF	diphthine synthase activity	5	0.0006262	9.03E-05
7	8629	BP	induction of apoptosis by intracellular signals	17	0.0006292	0.0060299
8	79	BP	regulation of cyclin-dependent protein kinase activity	30	0.0009682	0.0006918
9	8022	MF	protein C-terminus binding	28	0.0010178	0.0332401
10	30274	MF	LIM domain binding	5	0.0027241	0.0278159
11	17182	BP	peptidyl-diphthamide metabolism	8	0.0031029	0.001998
12	17183	BP	peptidyl-diphthamide biosynthesis from peptidyl-histidine	8	0.0031029	0.001998
13	18202	BP	peptidyl-histidine modification	8	0.0031029	0.001998
14	8428	MF	ribonuclease inhibitor activity	5	0.0031816	0.0130247

15	45815	BP	positive regulation of gene expression, epigenetic	7	0.0032192	0.0187543
16	43028	MF	caspase regulator activity	5	0.0035432	0.3403788
17	31202	MF	RNA splicing factor activity, transesterification mechanism	23	0.0042451	0.0013586
18	8757	MF	S-adenosylmethionine-dependent methyltransferase activity	76	0.0044728	0.0618698
19	7021	BP	tubulin folding	5	0.0046218	0.0028239
20	8013	MF	beta-catenin binding	7	0.0048826	0.0031594
21	118	CC	histone deacetylase complex	38	0.0080248	0.0020909
22	9897	CC	external side of plasma membrane	9	0.0085632	0.0021181
23	45736	BP	negative regulation of cyclin-dependent protein kinase activity	5	0.0182021	0.0028634
24	3747	MF	translation release factor activity	8	0.045947	0.0046691
25	8079	MF	translation termination factor activity	8	0.045947	0.0046691
26	42393	MF	histone binding	18	0.172388	0.0043185

[1] The 26 GO categories found to be significant at the nominal 0.005 level of the LS permutation test or KS permutation test (sorted by p-values of the LS permutation test). For each GO category, the table lists the unique identifier, the number of genes in the project gene list that belong to the GO category, and the LS and KS p-values. The presented GO categories are ordered by the p-value of the LS test (smallest first).
[2] Go-term: CC = cellular component, BP = biological process and MF = molecular function.
[3] Fisher (LS) statistic is defined as the mean negative natural logarithm of the p-values of the appropriate single gene univariate test.
[4] Kolmogorov-Smirnov (KS) statistic is used for testing if the p-values are of a uniform distribution.

Table 2B: Differentially expressed genes in GO categories between 18 sets of normal and atypical melanocytes

nr	GO Term[1]	GO description	Probe set	Description[2]	Gene symbol	Parametric p-values
1	CC	organellar ribosome	219220_x_at	mitochondrial ribosomal protein S22	MRPS22	0.0001097
2	CC	organellar ribosome	223480_s_at	mitochondrial ribosomal protein L47	MRPL47	0.000131
3	CC	organellar ribosome	218558_s_at	mitochondrial ribosomal protein L39	MRPL39	0.006304
4	CC	organellar ribosome	224869_s_at	mitochondrial ribosomal protein S25	MRPS25	0.0151834
5	CC	organellar ribosome	222775_s_at	mitochondrial ribosomal protein L35	MRPL35	0.0171902
6	CC	mitochondrial ribosome	219220_x_at	mitochondrial ribosomal protein S16	MRPS16	0.0005530
7	CC	mitochondrial ribosome	223480_s_at	mitochondrial ribosomal protein L44	MRPL44	0.000131
8	CC	mitochondrial ribosome	219819_s_at	mitochondrial ribosomal protein S28	MRPS28	0.0029398
9	CC	mitochondrial ribosome	217919_s_at	mitochondrial ribosomal protein L42	MRPL42	0.0303516
10	CC	mitochondrial ribosome	222993_at	mitochondrial ribosomal protein S37	MRPL37	0.003539
11	MF	hydrogen ion transporter activity	213846_at	cytochrome c oxidase subunit VIIc	COX7C	0.0020774
19	MF	hydrogen ion transporter activity	218484_at	NADH dehydrogenase (ubiquinone) 1	NDUFA4L2	0.00585351
12	MF	hydrogen ion transporter activity	238765_at	ATPase, H+ transporting, lysosomal 13kDa, V1 subunit G1	ATP6V1G1	0.0059421

				ubiquinol-cytochrome c reductase binding		
13	MF	hydrogen ion transporter activity	209065_at	protein	UQCRB	0.0171665
14	MF	hydrogen ion transporter activity	231487_at	cytochrome c oxidase subunit 8C	COX8C	0.021483
				ATPase, H+ transporting, lysosomal 31kDa, V1		
15	MF	hydrogen ion transporter activity	1552286_at	subunit E2	ATP6V1E2	0.0279023
16	MF	hydrogen ion transporter activity	202698_x_at	cytochrome c oxidase subunit IV isoform 1	COX4I1	0.0380242
				ubiquinol-cytochrome c reductase complex (7.2		
17	MF	hydrogen ion transporter activity	228142_at	kD)	UCRC	0.0389511
				membrane-spanning 4-domains, subfamily A,		
18	MF	hydrogen ion transporter activity	220834_at	member 12	MS4A12	0.0460068
20	CC	prefoldin complex	207132_x_at	prefoldin subunit 5	PFDN5	0.0086113
21	CC	prefoldin complex	218336_at	prefoldin subunit 2	PFDN2	0.0225808
22	CC	prefoldin complex	222019_at	prefoldin subunit 6	PFDN6	0.0326926
23	CC	prefoldin complex	201472_at	von Hippel-Lindau binding protein 1	VBP1	0.0345687
25	CC	prefoldin complex	205963_s_at	DnaJ homolog, subfamily A, member 3	DNAJA3	0.04568034
26	MF	oxidoreductase activity	207843_x_at	cytochrome b5 type A	CYB5A	0.01245134
27	MF	oxidoreductase activity	1560609_at	crystallin zeta (quinone reductase)-like 1	CRYZL1	0.0496658

28	BP	induction of apoptosis by intracellular signals	223828_s_at	lectin, galactoside-binding, soluble, 12 (galectin 12)	LGALS12	0.0004639
29	MF	cAMP-dependent protein kinase regulator activity	224191_x_at	ropporin, rhophilin associated protein 1	ROPN1	0.0065855
30	MF	cAMP-dependent protein kinase regulator activity	205406_s_at	sperm autoantigenic protein 17	SPA17	0.0110802

[1] The different GO-Terms: CC = cellular component; MF= molecular function; BP= Biological process.

[2] Genes found to be differentially expressed with a parametric p-value of less than 0.05 in the top 7 of GO categories. They are ordered by the parametric p-value associated with the GO category for each class.

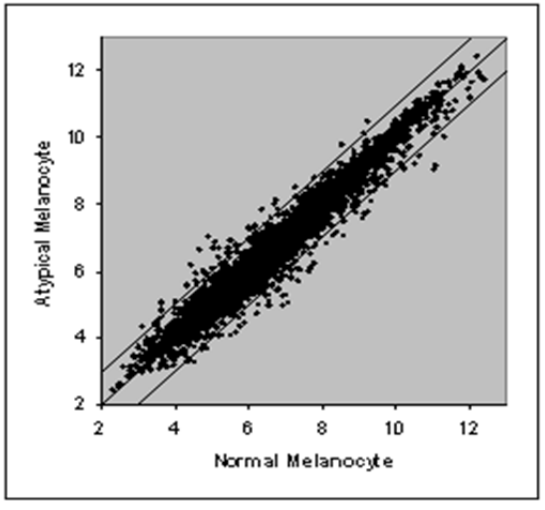

Fig1A

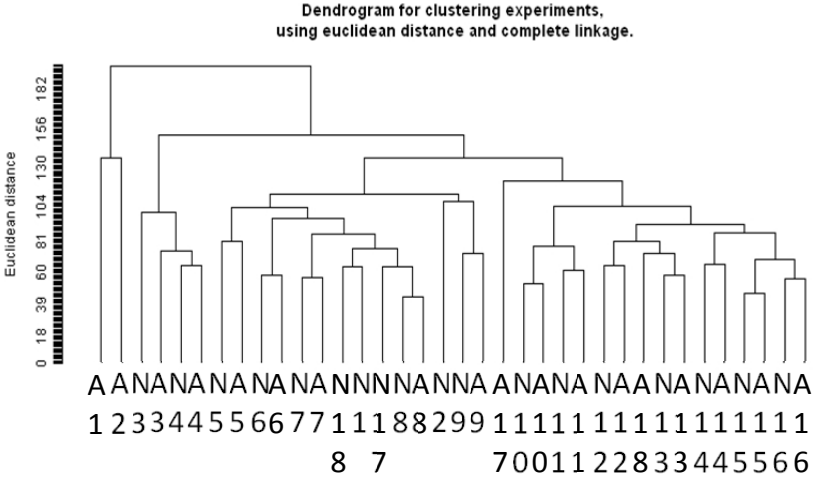

Fig1B

Fig 1: A. Scatter plot representing a set of normal and atypical melanocytes. Gene expression data was normalized with RMA method. On the x-as the gene expression of the normal melanocytes and on the Y-axis the gene expression of the corresponding atypical melanocyte is depicted. The small lines in the graph are the outlier lines and indicate a 2 fold-difference between the geometric mean of the expression ratios between normal and atypical melanocytes. Clearly visible is that the gene expression differences between normal and atypical melanocytes are small.

B. Dendogram of the normal and atypical melanocytes (A = atypical melanocyte and N = normal melanocyte). Most normal and atypical melanocytes of the same person cluster together indicating that the gene expression differences between the two samples are small and that the differences between individuals are larger. De bar on the y-axis depicts the Euclidean distance with complete linkage which is a measure on how similar samples are. Also the R-index (0.997) and D-index (0.02) were calculated to determine the robustness of the clusters (see material and methods) and showed that the clusters are highly reproducible.

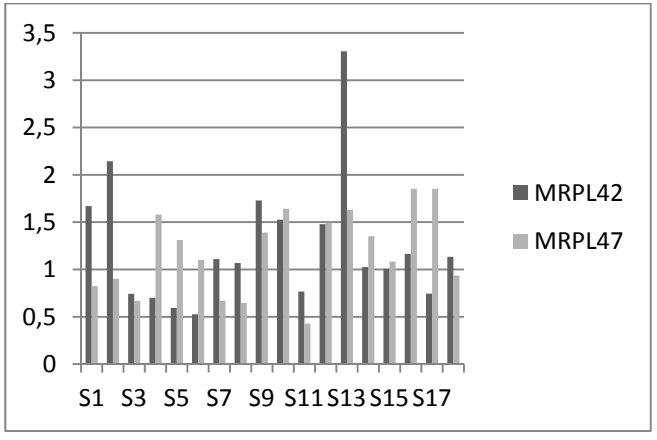

Fig 2: MRPS42 and MRPS47mRNA expression differences in normal and atypical melanocytes. On the x-axis the sets normal and atypical melanocytes are depicted by S1 till S18. Depicted on the y-axis is the ratio of the gene expression difference between normal and atypical melanocytes. A value lower than one indicates gene expression is lower in the atypical melanocyte in comparison with its normal counterpart. Both genes are representatives of the organellar and mitochondrial ribosome GO-categories.